Functional insights into nucleoside diphosphate kinases encoded by two *ndk* paralogs in *Waddlia chondrophila*

Giti Ghazi-Soltani, Carole Kebbi-Beghdadi, Simone E. Adams and Gilbert Greub*

Center for Research on Intracellular Bacteria, Institute of Microbiology, University Hospital Center and University of Lausanne, Lausanne, Switzerland

* Corresponding author: gilbert.greub@chuv.ch

ABSTRACT

The *Chlamydiota* phylum consists of obligate intracellular bacteria, including well-known pathogens and emerging environmental species, with diverse host ranges and metabolic capabilities. Among these bacteria, the gene, which encodes nucleoside diphosphate kinase (*ndk*), is present in variable copy numbers. While most chlamydial species carry a single copy of *ndk*, some species have two copies. In *W. chondrophila*, the two Ndk proteins encoded by *ndk* paralogs retain conserved kinase motifs but differ in subcellular localization, suggesting divergent functional roles. According to localization studies performed in heterologous expression systems, WcNdk1 is confined to the inclusion and probably supports nucleotide metabolism, while WcNdk2 localizes to the host nucleus, perinuclear space, and Golgi apparatus, suggesting involvement in host interaction. Azidothymidine (AZT), a known Ndk inhibitor, impaired *W. chondrophila* growth, potentially through inhibition of WcNdk2. However, the lack of genetic tools and the absence of *in vitro* enzymatic assays currently limit definitive functional conclusions. Our data suggest potential functions for Ndks in *W. chondrophila,* providing a foundation for future studies on Ndk-mediated interactions between this pathogen and its host.

Keywords: *Waddlia chondrophila*, Nucleoside diphosphate kinase (Ndk), AZT inhibition, Subcellular localization, Protein trafficking

INTRODUCTION

The *Chlamydiota* phylum encompasses several families of obligate intracellular bacteria, including six main families: *Chlamydiaceae*, *Parachlamydiaceae*, *Waddliaceae*, *Simkaniaceae*, *Rhabdochlamydiaceae*, and *Criblamydiaceae*. Members of these families share a biphasic developmental cycle, which reflects their adaptation to intracellular environments and reliance on host cell machinery for survival.

W. chondrophila belongs to the family *Waddliaceae* and is known as an abortigenic agent in ruminants. It was first isolated from an aborted bovine fetus[1,2] and serological studies showed a strong association between anti-*Waddlia* antibodies and bovine abortion[3]. In humans, *W. chondrophila* seropositivity is significantly associated with adverse pregnancy outcomes[4–6]. This pathogen was also detected in respiratory tract samples of patients with pneumonia and children with bronchiolitis[7,8].

The *W. chondrophila* developmental cycle is biphasic and is divided into three major phases[9,10]. In the early phase (0-8 hours post-infection, hpi) elementary bodies (EBs) enter in host cells and differentiate into reticulate bodies (RBs). This phase is followed by a proliferation phase (8-24 hpi) during which the number of RBs increases exponentially through binary fission. In the late phase (24 - 48 hpi), RBs revert into EBs and lysis of the host cell releases infectious progeny. Under environmental or antibiotic stress, the developmental cycle is arrested leading to an enlarged, non-dividing RB-like form called Aberrant Body (AB)[11]. While *W. chondrophila* significantly impacts both animal and human health, the specific molecular and genomic pathways, particularly those involving developmental and regulatory proteins, remain largely unexplored. Functional characterization of proteins, such as nucleoside diphosphate kinase (Ndk), could help us to better understand the biology and pathogenicity of this pathogen and its adaptation inside host cells.

Ndk is a highly conserved enzyme that plays a central role in maintaining nucleotide pools within both bacterial and eukaryotic cells. The maintenance of intracellular NTP pools is vital for the survival and proliferation of all living organisms. Ndk regulates nucleotide pools through its autophosphorylation and phosphotransferase activities. This ensures that NTP and dNTP levels remain balanced for optimal cellular function.

Beyond its housekeeping functions, Ndk is implicated in various cellular processes, including cell differentiation and development in eukaryotes and prokaryotes[12–15]. Additionally, Ndk is involved in the regulation of gene expression[16–18]. Due to its ability to bind ATP, Ndk is

62 involved in inhibiting extracellular ATP (eATP) and disrupting purinergic signaling in immune
63 and inflammatory responses[19–21].
64 We previously reported transcriptomic data for *W. chondrophila* comparing genes expression
65 in RBs at 24 hpi and EBs at 72 hpi[22]. In that dataset, both *ndk* genes were differentially
66 expressed between the two developmental stages, each showing a fold change of 0.3 in EBs
67 compared with RBs. Despite the well-established functions of Ndk across various organisms,
68 its specific function in the *Chlamydiota* remains uncharacterized. Based on these observations,
69 we hypothesized that this enzyme could play an important role in the development and
70 pathogenesis of *W. chondrophila*. In this study, we characterize the two Ndk proteins in this
71 organism to better understand their potential role in the bacterium's development. This study
72 provides an overall view of Ndk proteins in the *Chlamydiota* phylum and offers functional
73 insights into the Ndks proteins of *W. chondrophila*. Our results pave the way for more detailed
74 research once genetic tools become available for *W. chondrophila*.

75 RESULTS

76 Evolution of the *ndk* operon in the *Chlamydiota* phylum

77 Similar to other organisms, all bacteria of the *Chlamydiota* phylum possess at least one copy
78 of the *ndk* gene. A second copy (*ndk2*) is present in members of the *Parachlamydiaceae*,
79 *Waddliaceae*, and *Criblamydiaceae* families (Figure 1A). Interestingly, *ndk2* forms an operon
80 with the ancestral *ndk1* gene. In most species, this operon is further associated with *pabA*,
81 which encodes para-aminobenzoate synthase and is involved in the folate biosynthesis
82 pathway. Comparison of gene-based and species-based phylogenetic trees (Figure 1B, C)
83 suggests that the duplication of *ndk2* most likely originated from a single gene duplication
84 event in the common ancestor of the *Parachlamydiaceae*, *Waddliaceae*, and *Criblamydiaceae*.
85 However, a scenario of ancestral duplication with subsequent loss in *Simkaniaceae* and
86 *Chlamydiaceae* cannot be excluded, although it is less parsimonious.

87 High sequence and structural conservation of Ndk across species

88 The multiple sequence alignment shows a high degree of sequence conservation of Ndk
89 proteins from various bacterial and eukaryotic species (Figure 2A). Specifically, the His-Gly-
90 Ser-Asp (HGSD) motif, which is the enzyme's active site[23], is well conserved across all aligned
91 sequences. The highly conserved histidine residue inside this motif transiently receives the
92 phosphate group during autophosphorylation reaction and is, therefore, critical for the catalytic
93 function of Ndk. In addition to the HGSD motif, other conserved residues are observed in

94 regions associated with nucleotide binding and structural stability, many of which are enriched
95 in hydrophobic amino acids. These residues likely contribute to the proper folding and
96 enzymatic efficiency of Ndk.
97 *W. chondrophila* contains two copies of *ndk*: *wcndk1 (*locus *wcw_1543*) and *wcndk2* (locus
98 *wcw_1545*), with a sequence similarity of 54% (Figure 2B). The most striking difference
99 between the two *W. chondrophila ndk* paralogs is the presence of a predicted signal peptide of
100 17 amino acids in WcNdk2, which is absent in WcNdk1.
101 The sequence similarity matrix of *W. chondrophila* Ndk proteins, WcNdk1 and WcNdk2, and
102 their counterparts from other bacterial and eukaryotic species shows differing degrees of
103 conservation as shown in Figure 2B. WcNdk1 shares the highest sequence identity with *E. coli*
104 Ndk (EcNdk) and *Chlamydia trachomatis* Ndk (CtNdk) (67 % and 66%, respectively). In
105 contrast, WcNdk2 exhibits slightly lower sequence similarity across species, which may
106 indicate functional divergence of the two Ndks following gene duplication. Interestingly, both
107 *W. chondrophila* Ndk homologs display relatively high sequence identity (~50%) with human
108 Ndk (HsNdk), which suggests the conservation of core functional domains across vast
109 evolutionary distance. Sequence similarity matrix of Ndk proteins across different species is
110 shown in Table S2.
111 WcNdk1 has 143 residues forming a polypeptide chain and adopting a very similar fold to Ndk
112 protein from other origins including human Ndk[24,25] (Figure 2C). One Ndk unit has α/β
113 domains comprising a four-stranded antiparallel β-sheet and two connecting α-helices. This
114 high degree of sequence and structural conservation between eukaryotes and the pathogens
115 may enable them to interfere with host cellular process by mimicking host Ndk.

116 **Expression profile of *W. chondrophila* Ndks during infection**

117 Temporal expression levels of genes and proteins across different developmental stages may
118 help us understand their stage-specific roles and regulatory mechanisms. Since each of these
119 stages has unique biological features, we can indirectly infer a protein's function by mapping
120 both transcript and protein levels across these developmental stages.
121 We quantified the expression profiles of *W. chondrophila ndks*, at both the transcript and
122 protein level during McCoy cell infection (Figure 3). *wcndk1* and *wcndk2* transcripts were
123 highly abundant at early time points (3 - 8 hpi) as revealed by RT-qPCR, then the mRNA level
124 declined sharply to a minimum at 32 hpi, with a moderate surge toward the end of the cycle
125 (48 hpi) (Figure 3A). In parallel, protein expression profile of WcNdk1 or WcNdk2 were
126 analyzed using antibodies specifically raised against each protein. No WcNdk1 or WcNdk2

127 protein could be detected by Western blot of the *W. chondrophila*-infected cells at 3 to 8 hpi
128 (Figure 3B, C). Both proteins became detectable by 24 hpi by Western blot and reached their
129 highest signal intensity at this time point after normalization to bacterial number, followed by
130 a drop to roughly 30% of that level by 48 hpi. To further assess protein expression at early
131 stages, we performed immunofluorescence microscopy. In contrast to Western blot results,
132 WcNdk1 and WcNdk2 signals were already detectable from 0 to 16 hpi, colocalizing with *W.*
133 *chondrophila* (Figure S1). Together, these results suggests that both WcNdk1 and WcNdk2 are
134 expressed throughout the developmental cycle, with an early transcriptional peak. While
135 protein expression begins early, overall accumulation or detection sensitivity by Western blot
136 peaks around 24 hpi, followed by a decline toward the end of the cycle.

137 **Subcellular localization of WcNdk1 and WcNdk2 in *C. trachomatis* heterologous**
138 **expression**

139 While signal peptides are typically associated with protein secretion, previous studies have
140 demonstrated that Ndk can be secreted in certain bacterial species despite lacking a canonical
141 signal sequence[26–28]. Moreover, the secretion of both WcNdk1 and WcNdk2 into the host cell
142 cytoplasm is experimentally shown[29], suggesting that WcNdk2 signal peptide may not
143 contribute to secretion. The presence of a signal peptide on WcNdk2 suggests that it may be
144 translocated to a specific subcellular compartment, giving it a biological role distinct from
145 WcNdk1. To assess this possibility, we overexpressed a V5-tagged versions of WcNdk1 and
146 WcNdk2 in *C. trachomatis* using the inducible shuttle vector pGL2 (Unpublished) and studied
147 their subcellular localization by immunofluorescence and confocal microscopy (Figure 4). In
148 this heterologous expression assay, WcNdk1 was exclusively detected inside the inclusion,
149 closely associated with *C. trachomatis*, and no signal was observed in the host cell cytoplasm.
150 Although this does not rule out secretion of WcNdk1, it suggests limited accumulation or
151 detection outside the inclusion. In contrast, WcNdk2 was detected within both chlamydial
152 inclusions and the host-cell nucleus, suggesting its trafficking into the nucleus. To further
153 investigate the nuclear localization of WcNdk2, we cloned the gene into the pBOMBL vector[30]
154 and overexpressed the protein in *C. trachomatis*. Upon infection of McCoy cells with the
155 transformed bacteria, inclusions were smaller, and bacterial growth was impaired compared to
156 controls. Due to these growth defects, reliable localization of WcNdk2 could not be realized in
157 this system. This vector-associated toxicity likely reflects bacterial stress caused by excessive
158 or mis-regulated expression of WcNdk2, similar to the overexpression-associated toxicity
159 reported for type III effectors in *Pseudomonas aeruginosa*[31]. Consistently, WcNdk2 expression

160 was also not detected in the *Yersinia enterocolitica* type III secretion assay, suggesting poor
161 tolerance or instability of the protein in this system.

162 **Subcellular localization of WcNdk1 and WcNdk2 in transfected HEK293T cells**

163 To further confirm the observed subcellular localization of WcNdk1 and WcNdk2 in another
164 heterologous system, we transiently expressed the V5-tagged WcNdk1 and WcNdk2 in
165 HEK293T cells and analyzed their distribution by immunofluorescence microscopy. WcNdk1
166 was found exclusively in the cytoplasm and was absent from cell compartments such as nucleus
167 or Golgi (Figure 5). WcNdk2 showed two mutually exclusive distribution patterns. In some
168 cells the V5 signal was found throughout the nucleus, while in others, it was localized to
169 perinuclear-Golgi regions, with no nuclear signal (Figure 5). A similar localization of WcNdk2
170 was also observed in transfected HeLa cells (data not shown), indicating that this targeting is
171 not cell-type specific.

172 **The Ndk inhibitor, Azidothymidine (AZT), inhibits the growth of *W. chondrophila***

173 Since *W. chondrophila* is currently genetically intractable, we employed chemicals to inhibit
174 Ndk function in this pathogen. AZT (3′-azido-3′-deoxythymidine), also known as zidovudine,
175 is a known Ndk inhibitor[14,32–36]. This pharmaceutical, primarily approved for the treatment of
176 human immunodeficiency virus (HIV), inhibits viral reverse transcription through chain
177 termination[37]. This compound is structurally a thymidine analogue, where the 3'-hydroxyl
178 group on the deoxyribose sugar is replaced by an azido group (N_3) (Figure 6A).
179 The inhibition of the Ndk from *Aspergillus flavus* by AZT is documented, where AZT forms a
180 strong hydrogen bond with key active site residues of Ndk (Arg-104, His-117 and Asp-120)
181 and inhibits its enzymatic activity[14]. Since these three residues are highly conserved in Ndks
182 of diverse organisms, including WcNdk1 and WcNdk2, we hypothesized that AZT could also
183 serve as an effective inhibitor of Ndks in *W. chondrophila* (Figure 2A).
184 To test this hypothesis, we treated both uninfected and *W. chondrophila*-infected McCoy cells
185 with increasing concentrations of AZT following infection and measured cell death resulting
186 from bacterial proliferation using propidium iodide (PI) staining. In the absence of AZT or at
187 low concentrations (1 µg/ml), *W. chondrophila*-infected cultures exhibited a sharp increase in
188 cell mortality over time, reaching maximal levels by 144 hpi. Treatment with AZT at
189 concentrations above 25 µg/ml significantly suppressed infection-induced cell death. A delay
190 in cell mortality was observed with the intermediate concentration of 5 µg/ml (Figure 6B, right
191 panel). In contrast, in uninfected cells, cell lysis remained comparable across all AZT

192 concentrations, showing no significant difference from the no-AZT control. Therefore, the
193 slight increase in cell death observed over time in untreated cultures is due to normal cell aging
194 and turnover, and not due to AZT (Figure 6B, left panel). These results indicate that AZT did
195 not exhibit significant adverse effects on mammalian host cells and provided a protective effect
196 against *W. chondrophila*-induced cell death in a dose-dependent manner.

197 **Only early AZT treatment prevents *W. chondrophila*–mediated host cell death**

198 To define the temporal window in which AZT exhibits its inhibitory effect on *W. chondrophila*
199 growth, *W. chondrophila*-infected McCoy cell monolayers were treated with 25 µg/ml AZT at
200 0, 3, 8, 24, 32, or 48 hpi and the propidium iodide (PI) uptake was monitored at 24, 48, 72, and
201 144 hpi (Figure 6C). When AZT was added at 0, 3, or 8 hpi, cell mortality remained minimal
202 (approximately 25% at 144 hpi), comparable to uninfected controls, indicating complete
203 protection against bacterial-induced cell death. In contrast, administering AZT at 24 hpi or later
204 failed to prevent cell death, resulting in maximal mortality, comparable to the no-AZT control.
205 This indicates that once RB replication and inclusion expansion are established, AZT cannot
206 reverse the course of infection.

207 **AZT induced the production of aberrant bodies (ABs) in *W. chondrophila***

208 To investigate the cellular-level effects of AZT treatment on *W. chondrophila* infection, we
209 performed confocal microscopy on *W. chondrophila*-infected McCoy cells treated with 25
210 µg/ml AZT at 0 hpi. In untreated cultures, *W. chondrophila* underwent normal intracellular
211 development, leading to host cell lysis at the end of infection. At 8 hpi, *W. chondrophila* EBs
212 were observed attached to the host cell surface and internalized in both AZT-treated and
213 untreated cultures indicating that AZT does not interfere with bacterial attachment or entry
214 (Figure 6D). By 24 hpi, inclusions had formed in both conditions. However, in AZT-treated
215 cells, these inclusions failed to expand, and only a limited number of bacteria were detected
216 within them. This suggests that although EB-to-RB differentiation and initial rounds of
217 replication may occur, bacterial proliferation is subsequently arrested. In addition, the *W.*
218 *chondrophila* RBs appeared slightly enlarged in AZT-treated cultures, consistent with the
219 formation of aberrant bodies (ABs). These abnormal conditions persisted until 72 hpi,
220 indicating a disruption of the normal developmental cycle likely resulting in bacterial
221 persistence.

222 **Effect of AZT on *W. chondrophila* growth is probably correlated with WcNdk2 activity**

223 *W. chondrophila* encodes two *ndk* paralogs, organized in a single operon, with *pabA* positioned
224 between them. To investigate which *ndk* copy mediates susceptibility to AZT, and whether this

225 susceptibility is linked to the presence of the *pabA* gene, we selected representative
226 *Chlamydiota* species with different *ndk* operon configurations and compared their response to
227 AZT treatment. The selected species include *C. trachomatis*, which carries a single *ctndk* gene
228 and lacks *pabA*; *Simkania negevensis,* which also has a single *snndk* gene but retains *pabA*
229 elsewhere in the genome; *Estrella lausannensis*, which harbors a two-gene *elndk1–elndk2*
230 operon without *pabA*; and *W. chondrophila*, which contains the full *wcndk1–pabA–wcndk2*
231 operon (Figure 7, bottom panel). To evaluate the effect of AZT on these species, McCoy cell
232 monolayers were infected, treated with 25 µg/ml at 0 hpi and fixed at 48 hpi before
233 immunostaining and observation under confocal microscopy. As shown in Figure 7C,
234 *trachomatis* and *S. negevensis* exhibited normal intracellular development in presence of AZT,
235 indicating no significant growth inhibition. In contrast, *E. lausannensis*, like *W. chondrophila*,
236 displayed enlarged intracellular structures resembling aberrant bodies. This suggest that AZT
237 inhibitory effect depends on the presence of *ndk2*, regardless of the presence of *ndk1* and *pabA*.

238 DISCUSSION

239 The diversity of *ndk* copy number within members of the *Chlamydiota* reveals lineage-specific
240 adaptations with potential metabolic and pathogenic consequences. While most *Chlamydiota*
241 species possess a single *ndk* gene, a subset, including members of the *Parachlamydiaceae*,
242 *Waddliaceae*, and *Criblamydiaceae*, harbor a second copy (*ndk2*), likely arising from a gene
243 duplication event. This duplication may have provided a selective advantage by providing
244 increasing metabolism flexibility, which could, in part, account for the comparatively faster
245 growth of *W. chondrophila* and *E. lausannensis* in mammalian cells relative to other members
246 of the *Chlamydiota* such as *Chlamydia* spp. and *S. negevensis*. Such an expansion of metabolic
247 capacities might also represent an adaptation facilitating persistence and replication within
248 free-living protists, suggesting that these lineages have evolved mechanisms enabling survival
249 across diverse host environments. This is in line with their larger genome size (>2 Mb),
250 expanded metabolic genes and their reduced dependence on host-derived metabolites. On the
251 other side, the absence of the second copy of the *ndk* gene in *Rhabdochlamydiaceae*,
252 *Simkaniaceae* and *Chlamydiaceae* coincides with their adaptations to more specific host niches
253 and reduced metabolic pathways. The *pabA* gene is also absent in all members of the
254 *Chlamydiaceae* family. In this family, enzymes from other biosynthetic pathways are recruited
255 to meet their folate requirements[38]. The mechanisms driving the evolution of this operon in

256 certain chlamydial families remains unknown. Further studies are needed to clarify the
257 operon's functional role and its evolutionary pathways in these families.

258 Both *W. chondrophila ndk* paralogs retain the universally conserved HGSD active-site motif
259 and surrounding hydrophobic residues essential for autophosphorylation and
260 phosphotransferase activities. This conservation suggests that both Ndk1 and Ndk2, despite
261 their apparent different subcellular localizations, exert their functions, at least partially, through
262 phosphorylation mechanisms.
263 The temporal expression patterns of *wcndk1* and *wcndk2* provide insights into their potential
264 biological roles and regulation during the *W. chondrophila* developmental cycle. The
265 organization of *wcndk1* and *wcndk2* within a single operon explains their synchronized
266 expression profiles. The apparent mid-cycle surge in Ndk protein at 24 hpi coincides with the
267 maximal bacterial replication, an increased demand for NTPs, and an increased host-
268 manipulation activities that are essential for intracellular growth.
269 Despite sharing conserved kinase domains, our study showed significant differences in
270 subcellular localization of WcNdk1 and WcNdk2. This divergence suggests functional
271 specializations and may indicate that the two proteins utilize divergent cellular trafficking
272 mechanisms during *W. chondrophila* infection.
273 In the *C. trachomatis* expression system, WcNdk1 was confined to the inclusion. This restricted
274 distribution suggests that WcNdk1 may primarily serve bacterial intracellular functions within
275 the inclusion. However, a previous study provided evidence for the secretion of WcNdk1 into
276 the host cell cytosol[29]. It is, therefore, possible that WcNdk1 is secreted transiently or at levels
277 insufficient to be detected via immunofluorescence. In contrast, WcNdk2 exhibited nuclear
278 localization in *C. trachomatis* and HEK293T expression systems. This nuclear localization is
279 consistent with previous studies on other pathogens, where Ndk was shown to bind host DNA
280 and regulate gene expression through DNA cleavage[17,18]. Such putative nuclear activity
281 suggests a potential role for WcNdk2 in reprogramming host transcriptional responses to favor
282 bacterial survival or pathogenicity. It would be of great interest to identify specific host genes
283 targeted by WcNdk2, as this could uncover previously unrecognized mechanisms by which *W.*
284 *chondrophila* manipulates host cell function and could provide broader insights into its
285 pathogenesis.
286 When expressed in HEK293T cells, WcNdk2 localized not only to the nucleus but also to the
287 perinuclear-Golgi region. Bacterial Ndks, such as *Porphyromonas gingivalis* Ndk, are found
288 in the perinuclear area of the host cells. This localization has been linked to the modulation of

host purinergic signaling via $P2X_7$ receptors[28], implying that the perinuclear localization of WcNdk2 could be a biologically relevant phenomenon rather than nonspecific aggregation. Unlike the perinuclear accumulation of bacterial Ndks, Golgi localization represents a novel observation not previously reported for any bacterial species. One plausible explanation for an association of WcNdk2 with the Golgi is that, after translocation into the host cytosol, WcNdk2 enters the classical ER–Golgi secretory pathway and is packaged into Golgi-derived vesicles for extracellular release to hydrolyze host extracellular ATP (eATP) and subvert purinergic signaling. Another possible explanation for the Golgi recruitment of WcNdk2 is that it might play a role in modulating vesicle trafficking between the Golgi and the bacterial inclusion. Although *W. chondrophila* does not redirect sphingomyelin transport from the Golgi to its inclusion[39], it may still influence other aspects of vesicular trafficking, altering vesicle formation or fusion processes, to benefit bacterial survival or replication.

AZT is a well-established inhibitor of Ndk[14,32–36]. In our study, AZT treatment of *W. chondrophila*-infected cells protected them from bacteria-induced cell death and bacterial growth was arrested in the replication phase. Our comparative data across *Chlamydiota* species suggest that WcNdk2 is a potential target for AZT. WcNdk2 localizes to host cell compartments when expressed in heterologous systems and this positioning may increase its exposure to AZT. Thus, the growth arrest caused by AZT may result from disruption of Ndk2-dependent pathogenic mechanisms required for successful host-cell manipulation. Our results also showed that AZT must be applied before 24 hpi, to fully prevent *W. chondrophila*–induced cytotoxicity. This early phase of infection coincides with maximum RB replication, inclusion expansion, and active vesicular nutrient trafficking from the Golgi and ER[40]. In contrast, WcNdk1, which predominantly localizes within the bacteria, and is likely involved in maintaining bacterial nucleotide pools, appears less susceptible to AZT, possibly due to limited drug access to the inclusion compartment. These findings collectively support a model in which the inhibition of host-targeted, secreted WcNdk2, rather than the inclusion-confined WcNdk1, plays the key role in AZT's antimicrobial activity against *W. chondrophila*.

Based on these observations, we propose a functional model for the two *W. chondrophila* Ndks, as illustrated in Figure 8. Together, these findings highlight the multifunctional nature of Ndk proteins and shed light on the distinct roles of *W. chondrophila* Ndks. However, the lack of genetic manipulation tools in *W. chondrophila* currently impedes direct investigation of Ndk function via gene deletion or mutagenesis. Although localization studies using heterologous expression systems suggest that WcNdk2 may interact with host cells, the possibility of

322 overexpression artifacts or mis-localization cannot be entirely ruled out. Additionally, although
323 AZT is a well-established Ndk inhibitor with no other known bacterial targets, direct in vitro
324 evidence confirming WcNdk2 as the AZT target is still missing. In vitro ATPase assays are
325 essential to validate this interaction. In the absence of such studies the proposed functions
326 remain speculative. The advancement of genetic tools would be essential to validate the
327 proposed roles of WcNdk1 and WcNdk2 in *W. chondrophila* metabolism and host interaction.

328 CONCLUSION

329 Given its diverse activities, Ndk has attracted interest across multiple disciplines, including
330 microbiology, cell biology, and drug development. In this study, we introduced chlamydial Ndk
331 as a multifunctional protein with roles extending beyond nucleotide metabolism, highlighting
332 its potential involvement in host–pathogen interactions. These findings not only enhance our
333 understanding of Ndk biology in the *Chlamydiota* phylum but also point to Ndk2 as a potential
334 therapeutic target, opening new avenues for dissecting host manipulation strategies in obligate
335 intracellular bacteria.

336 MATERIALS AND METHODS

337 Phylogenetic and structural analysis

338 Species-based and *ndk* gene phylogenies were retrieved from the *Chlamydia* Database[41]. Trees
339 were trimmed using FigTree (v1.4.4) to retain only relevant *Chlamydiota* species. The Ndk
340 protein sequences across different taxa were retrieved from the National Center for
341 Biotechnology Information (NCBI). Multiple sequence alignment of Ndk proteins across
342 eukaryotes and prokaryotes was performed using the ClustalW tool in UGENE v1.30.0. The
343 corresponding similarity heat map (percentage identity, excluding gap) was also generated on
344 UGENE. Alignment visualization was carried out with EPSript
345 https://espript.ibcp.fr/ESPript/cgi-bin/ESPript.cgi. The 3D structure of the protein was
346 reconstructed using Phyre2[42] and visualized using Jmol v.16.2.15.

347 Cell culture and *W. chondrophila* infection

348 McCoy (murine fibroblast cells; ATCC CRL-1696, purchased from ATCC), HEK293T (ATCC
349 CRL-11268, USA, obtained as a gift from Dr. Thierry Roger, Lausanne University Hospital)
350 or HeLa cells (human cervical adenocarcinoma epithelial cells; ATCC CCL-2, a gift from Dr.
351 Thierry Roger) were maintained at 37°C in 5% CO_2 in DMEM GlutaMAX (Thermo Fisher

352 Scientific, USA), supplemented with 10% fetal bovine serum (FBS; Thermo Fisher Scientific,
353 USA). *W. chondrophila* (ATCC VR-1471) was propagated in *Acanthamoeba castellanii*
354 (ATCC 30010) at 25°C in T-25 flasks containing 6 ml of peptone–yeast–extract–glucose broth.
355 At the time of infection, lysed *W. chondrophila*-infected amoebae were filtered through a 5-
356 μm syringe filter to remove amoebal debris. The bacterial solution was then used to infect the
357 host cells at a dilution which was optimum for infection (MOI 0.1–1). To synchronize the
358 infection, the infected cells were centrifuged at 1790 g for 10 minutes. They were then
359 incubated at 37°C in 5% CO_2 for 15 minutes. Following incubation, the inoculum was then
360 replaced with fresh medium.

361 **Purification of recombinant His-tagged WcNdk1 and WcNdk2 for antiserum production**
362 The *E. coli* strain BL21 containing pET28a-*wcndk1-6xHis* or pET28a-*wcndk2-6xHis* was
363 grown to an OD_{600} of 0.5. The culture was induced using 1 mM Isopropyl β-D-
364 thiogalactopyranoside (IPTG, Applichem, Germany) and incubated at 37°C for 4 hours to
365 express the recombinant protein. Bacterial pellets were resuspended in native lysis buffer (50
366 mM NaH_2PO_4, 300 mM NaCl, and 10 mM imidazole, pH 8). The resuspended cells were lysed
367 using a combination of methods: three cycles of freeze (ethanol-dry ice bath) and thaw (at
368 37°C), followed by chemical lysis with 1 mg/ml lysozyme (AppliChem, Germany) and
369 sonication. The recombinant protein was purified under native condition using Ni-NTA agarose
370 beads (Qiagen, Germany) according to the manufacturer's instructions. Briefly, bacterial
371 lysates were incubated with Ni-NTA resin for 2 hours at 4 °C with gentle rotation. The protein-
372 bound resin was then loaded onto poly-prep chromatography columns (Bio-Rad, USA),
373 washed with wash buffer (50 mM Tris-HCl, 300 mM NaCl, 20 mM imidazole, pH 8.0), and
374 eluted with elution buffer containing 250 mM imidazole. The purified protein was dialyzed
375 using Slide-A-Lyzer Dialysis Cassette, 2,000 MWCO (Thermo Scientific, USA) overnight
376 against PBS to remove imidazole. The concentration of the protein was determined using
377 Bradford's reagent with BSA (Bio-Rad, USA) as a standard. Following protein purification,
378 rabbit polyclonal antisera were produced using immunization services offered by Eurogentec
379 SA (Seraing, Belgium).

380 **Western Blot**
381 McCoy cells were seeded at a density of 1 x 10^6 per T-25 flask one day before infection and
382 infected with *W. chondrophila* as described above. Infected cells were harvested by scraping at
383 the specified hpi and a fraction of the culture was saved for extraction and quantification of the
384 genomic DNA (see below). The cell suspension was pelleted at 1790 g for 10 minutes, then

385 washed twice with PBS, and finally resuspended in 0.5 ml of 1x Laemmli sample buffer (Bio-
386 Rad, USA). An equal volume of each lysate was resolved on 12% SDS-PAGE precast gels
387 (Bio-Rad, USA) and transferred onto an Amersham Protran nitrocellulose membrane (Cytiva,
388 USA). The membrane was blocked in saturation buffer (10 mM Tris-Base, 150 mM NaCl, and
389 0.05% Tween 20) containing 5% nonfat dried milk (AppliChem, Germany) for 2 hours at room
390 temperature (RT). Blots were probed overnight at 4°C with antibodies against WcNdk1 and
391 WcNdk2 diluted in saturation buffer with 0.5% non-fat dried milk. After three washes with
392 saturation buffer containing 0.5% non-fat dried milk, blots were incubated with secondary
393 antibodies (horseradish peroxidase-conjugated anti-rabbit IgG; Promega, USA, or anti-mouse
394 IgG; Bio-Rad, USA) for 1 hour at Room temperature and processed using the Amersham ECL
395 detection system (Cytiva, USA). Western blot bands intensities were quantified using
396 EvolutionCapt edge software (Vilber, France) and normalized to the corresponding bacterial
397 genome copy number. Graphs were generated using GraphPad v. 10.4.1.

398 **Extraction of genomic DNA and quantification of *W. chondrophila* genome copy number**
399 Genomic DNA from collected samples was extracted using the Wizard SV Genomic DNA
400 purification system (Promega, USA) according to the manufacturer's instructions. The
401 extracted DNA served as a template for qPCR with iTaq Universal Probes Supermix (Bio-Rad,
402 USA) to quantify the *W. chondrophila* bacterial population. The 16S copy numbers were
403 determined using a standard curve, which was generated from serial dilutions of a plasmid
404 containing one copy of the 16S rRNA gene. The primer sequences[8] are listed in Table S1.

405 **RNA extraction and cDNA synthesis**
406 *W. chondrophila*-infected McCoy cell monolayers or uninfected control cells were harvested
407 at indicated hpi by scraping and centrifugation (5000 g, 10 minutes). Following centrifugation
408 cells were lysed directly in TRIzol Reagent (Invitrogen, USA). Total RNA was extracted by
409 chloroform separation and recovery of the aqueous phase (12,000 g, 15 min, 4 °C). RNA was
410 precipitated with isopropanol, washed with 75 % ethanol, air-dried, and resuspended in
411 RNase-free water. To remove genomic DNA, samples were treated with RNase-free DNase I
412 (Invitrogen, USA) following the manufacturer's instructions. cDNA was synthesized using the
413 GoScript Reverse Transcription System (Promega, USA) with random primers. Reverse
414 transcription was performed at 42°C for 60 minutes, followed by enzyme inactivation at 70°C
415 for 15 minutes. All cDNAs were diluted 1:5 prior to qPCR.

416 **RT-qPCR**

417 The qPCR reactions were set up in a final volume of 20 µl containing 4 µl of cDNA template,
418 the appropriate concentration of each primer, and 1X iTaq Universal SYBR Green Supermix
419 (Bio-Rad, USA). All samples were run in duplicates, and no-template controls were included
420 for each primer pair to assess non-specific amplification. The fluorescent reporter signal was
421 normalized against the internal reference dye (ROX) signal. qPCR was carried out on
422 QuantStudio 3 Real-Time PCR System (Applied Biosystems, USA) using the following
423 thermal program. A single cycle of DNA polymerase activation for 3 min at 95 °C, followed
424 by 45 amplification cycles of 15 s at 95 °C (denaturing step) and 1 min at 60 °C (annealing and
425 extension step). Gene expression data were normalized to *W. chondrophila* 16 rRNA gene,
426 which served as the internal reference gene. Quantitative data from qRT-PCR experiments were
427 collected from at least three independent replicates. The primers used for RT-qPCR are listed
428 in Table S1.

429 **Application of AZT on *W. chondrophila* culture and cell death assessment**

430 McCoy cells were seeded at a density of 1×10^4 cells per well in 96-well plates (Corning,
431 USA). Cells were infected with *W. chondrophila* or left uninfected as a control. To monitor cell
432 death, Propidium Iodide (PI, 7 µg/mL, Sigma-Aldrich, Germany) was added to the growth
433 medium. AZT was purchased from TOCRIS (Cat. No.:4150) and was added to the wells at
434 concentrations ranging from 0 to 250 µg/mL in six technical replicates per condition.
435 Depending on the experimental design, AZT was added at the time of infection (0 hpi) or at
436 later time points (3, 8, 24, 32, and 48 hpi). PI fluorescence was measured at specified time
437 points post-infection using a FLUOstar Omega plate reader (BMG LABTECH, Germany;
438 excitation: 540 nm; emission: 640 nm). To define 100% cell death, 0.1% Triton X-100 was
439 added to control wells prior to PI reading.

440 **Antibodies, immunofluorescence assay, and confocal microscopy**

441 Mouse anti-V5 antibody were purchased from Thermo Fisher Scientific (USA). Goat anti-
442 *Chlamydia trachomatis* major outer membrane protein (MOMP) antibodies were obtained
443 from Lifespan Bioscience (LS-C55983, USA). Polyclonal antibodies against *W.*
444 *chondrophila*, *E. lausannensis*, and *S. negevensis* were homemade. Antibodies against GM130
445 (a cis-Golgi marker) were obtained from BD Biosciences (USA). Secondary anti-mouse, and
446 anti-rabbit or anti-goat antibodies conjugated to Alexa Fluor 488 or 594, as well as Texas Red–
447 conjugated concanavalin A, were purchased from AppliChem (Germany).

448 McCoy cells were cultured on glass coverslips placed in 24-well-plates and infected with
449 various bacterial species. At the indicated time points, cells were fixed with ice-cold methanol
450 or 4% paraformaldehyde (PFA) for 5 minutes at 4°C, followed by three washes with phosphate-
451 buffered saline (PBS). Fixed cells were permeabilized and blocked for 30 minutes using a
452 blocking solution containing 0.1% saponin, 10% fetal bovine serum (FBS), and 0.04% sodium
453 azide in PBS. Blocked cells were incubated with primary antibodies for 2 hours at RT (anti-V5
454 diluted 1:5000, anti-MOMP diluted 1:500 and anti GM130 diluted 1:300). After three washing
455 steps with blocking solution, cells were incubated for 1 hour with Alexa Fluor 488- or 598-
456 conjugated secondary antibodies (1:1000 dilution) to label bacteria. DAPI (4′,6-diamidino-2-
457 phenylindole; Thermo Fisher Scientific, USA) (1:3000 dilution) and Concanavalin A (1:50
458 dilution) were used to stain nuclei and carbohydrates, respectively. Cells were then washed
459 three times with PBS and briefly rinsed with purified water before mounting. Coverslips were
460 mounted on glass slides with Mowiol 4-88 (Sigma-Aldrich, USA) and stored in the dark until
461 imaging using Zeiss (LSM 900, Germany) confocal laser scanning microscope.

462 **pGL2 and pBOMBL plasmid construction**

463 The genes *wcndk1* and *wcndk2* were amplified from *W. chondrophila* genomic DNA using
464 primers with 5′ overhangs compatible with the pGL2 (a kind gift from the Scott Hefty
465 laboratory, University of Kansas) or pBOMBL (generously provided by Scot Ouellette
466 laboratory, University of Nebraska Medical Center) backbone. All PCR products included a C-
467 terminal V5 epitope tag to facilitate detection. PCR products were purified using the QIAquick
468 PCR Purification Kit (Qiagen, Germany). The pBOMBL vector was linearized with EagI and
469 KpnI (NEB, USA). The native *C. trachomatis*–derived pGL2 vector (11,786 bp; β-lactamase
470 selection marker) was linearized by Age I digestion (NEB, USA) and recovered from agarose
471 gels with the QIAquick Gel Extraction Kit (Qiagen, Germany). Purified inserts and linearized
472 vectors were assembled via In-fusion cloning using 5X In-fusion Snap assembly Master Mix
473 (Takara Bio, Japan). Assemblies were incubated at 50 °C for 15 min. Transformations were
474 performed using *E. coli* dam^- dcm^- cells. Positive clones were screened by colony PCR, and
475 successful insertions were confirmed by Sanger sequencing using both vector- and insert-
476 specific primers.

477 ***C. trachomatis* transformation**

478 Transformation of *C. trachomatis* was performed with minor modifications to previously
479 described methods[43].1 x 10^6 McCoy cells were seeded in 6-well plates and cultured overnight.
480 2.5 x 10^6 plasmid-free *C. trachomatis* serovar L2 (EBs), were resuspended in 300µl Tris-$CaCl_2$

481 buffer (10 mM Tris, 50 mM CaCl2, pH 7.4), and incubated with 2 µg of sequence-verified
482 plasmid DNA for 30 minutes at room temperature. 1 mL Hank's balanced salt solution (HBSS;
483 Gibco, Thermo Fisher Scientific, USA) was then added to each reaction. This mixture was
484 added to McCoy cells in a 6-well plate after removing the medium. The infection was carried
485 out by centrifugation at 400 × g for 15 minutes at room temperature and incubation at 37°C for
486 15 minutes. Then, the inoculum was removed, and cells were incubated with 2 mL of DMEM
487 medium supplemented with 10% FBS for 8 hours at 37°C and 5% CO_2. After this incubation,
488 the medium was replaced with DMEM containing 10% FBS, 1 µg/mL cycloheximide (Sigma-
489 Aldrich, Germany), and penicillin G (0.6 mg/mL; Sigma-Aldrich, Germany) or spectinomycin
490 (50 µg/mL; Sigma-Aldrich, Germany) to select for transformed bacteria. Cells were passaged
491 every 48 hours, and the development of fluorescent inclusions were monitored until they were
492 clearly observed and established. The transformed *C. trachomatis* was harvested and titrated
493 by IFU assay and stored at -80°C. For experiments requiring induction, 50 ng/ml
494 anhydrotetracycline (aTc, Sigma-Aldrich, Germany) was added at the time of infection,
495 whereas, in control conditions, the inducer was excluded.

496 **Gateway cloning for mammalian expression in pDEST47**

497 For generation of pDEST47 expression plasmids, attB-flanked primers were used to amplify
498 the C-terminal v5-tagged *wcndk1* and *wcndk2*. Entry clones were generated by BP
499 recombination using the Gateway BP Clonase II Enzyme Mix (Thermo Fisher Scientific,
500 USA). The resulting pDONR201-*ndk-v5* entry clones were selected on Kanamycin
501 (AppliChem, Germany) plates. Destination vectors were generated via LR recombination of
502 the entry clones with pDEST47 using the Gateway LR Clonase II Enzyme Mix (Thermo Fisher
503 Scientific, USA) following the supplier's instructions. Final constructs were transformed and
504 validated as described above, with plasmid DNA prepared from overnight cultures using the
505 GeneJET Plasmid Miniprep Kit (Thermo Fisher Scientific, USA).

506 **Transient transfection of HEK293T and HeLa cells**

507 Glass coverslips placed in 24-well plates were coated with poly-L-lysine (100 µg/mL; Sigma-
508 Aldrich, Germany) for 30 min at room temperature, washed three times with PBS, and air-
509 dried for 3 h. HEK293T cells were seeded on coated coverslips at 2×10^5 cells per well and
510 incubated overnight at 37 °C in 5 % CO_2. HeLa cells were seeded on uncoated coverslips at
511 2.5×10^5 cells per well and incubated under the same conditions. Twenty-four hours post-
512 seeding, cells were transfected with pDEST47 expression plasmids using the Lipofectamine
513 3000 Transfection Kit (Thermo Fisher Scientific, USA). according to the manufacturer's

514 instructions. Briefly, for each well, 1 μg plasmid DNA was diluted in 25 μL serum-free DMEM
515 containing 1 μL P3000 reagent. Separately, 0.75 μL Lipofectamine 3000 reagent was diluted
516 in 25 μL serum-free DMEM. The two mixtures were combined, incubated for 15 min at room
517 temperature, and 50 μL of the transfection complex was added dropwise per well. Cells were
518 fixed 24 hours post-transfection with PFA 4% for downstream immunofluorescence analysis
519 as described above.

COMPETING INTERESTS

The authors declare no competing interests.

AUTHOR CONTRIBUTIONS

G.G.S.: Conceptualization, Methodology, Investigation, Formal analysis, Visualization, Writing – original draft.

K.K.B.: Investigation, Validation, Resources, Writing – review & editing.

S.E.A.: Validation (pBOMBL-based experiment), Writing – review & editing.

G.G.: Supervision, Conceptualization, Project administration, Funding acquisition, Writing – review & editing.

FUNDING

This work was supported by the Swiss National Science Foundation (SNSF) [Grant No. 197768].

REFERENCES

1. Dilbeck PM, Evermann JF, Crawford TB, et al. Isolation of a previously undescribed rickettsia from an aborted bovine fetus. *J Clin Microbiol*. 1990;28(4):814-816.

2. Henning K, Schares G, Granzow H, et al. *Neospora caninum* and *Waddlia chondrophila* strain 2032/99 in a septic stillborn calf. *Veterinary Microbiology*. 2002;85(3):285-292. doi:10.1016/S0378-1135(01)00510-7

3. Dilbeck-Robertson P, McAllister MM, Bradway D, Evermann JF. Results of a new serologic test suggest an association of *Waddlia chondrophila* with bovine abortion. *J Vet Diagn Invest*. 2003;15(6):568-569. doi:10.1177/104063870301500609

4. Baud D, Thomas V, Arafa A, Regan L, Greub G. *Waddlia chondrophila*, a Potential Agent of Human Fetal Death. *Emerg Infect Dis*. 2007;13(8):1239-1243. doi:10.3201/eid1308.070315

5. Baud D, Goy G, Osterheld MC, et al. *Waddlia chondrophila*: from bovine abortion to human miscarriage. *Clin Infect Dis*. 2011;52(12):1469-1471. doi:10.1093/cid/cir205

6. Baud D, Regan L, Greub G. Emerging role of Chlamydia and Chlamydia-like organisms in adverse pregnancy outcomes. *Curr Opin Infect Dis*. 2008;21(1):70-76. doi:10.1097/QCO.0b013e3282f3e6a5

7. Haider S, Collingro A, Walochnik J, Wagner M, Horn M. Chlamydia-like bacteria in respiratory samples of community-acquired pneumonia patients. *FEMS Microbiol Lett*. 2008;281(2):198-202. doi:10.1111/j.1574-6968.2008.01099.x

8. Goy G, Croxatto A, Posfay-Barbe KM, Gervaix A, Greub G. Development of a real-time PCR for the specific detection of *Waddlia chondrophila* in clinical samples. *Eur J Clin Microbiol Infect Dis*. 2009;28(12):1483-1486. doi:10.1007/s10096-009-0804-7

9. de Barsy M, Greub G. *Waddlia chondrophila*: from biology to pathogenicity. *Microbes and Infection*. 2013;15(14):1033-1041. doi:10.1016/j.micinf.2013.09.010

10. Kebbi-Beghdadi C, Cisse O, Greub G. Permissivity of Vero cells, human pneumocytes and human endometrial cells to *Waddlia chondrophila*. *Microbes and Infection*. 2011;13(6):566-574. doi:10.1016/j.micinf.2011.01.020

11. Scherler A, Jacquier N, Kebbi-Beghdadi C, Greub G. Diverse Stress-Inducing Treatments cause Distinct Aberrant Body Morphologies in the Chlamydia-Related Bacterium, *Waddlia chondrophila*. *Microorganisms*. 2020;8(1):89. doi:10.3390/microorganisms8010089

12. Timmons L, Shearn A. Role of AWD/Nucleoside Diphosphate Kinase in Drosophila Development. *J Bioenerg Biomembr*. 2000;32(3):293-300. doi:10.1023/A:1005545214937

13. Masoudi N, Fancsalszky L, Pourkarimi E, et al. The NM23-H1/H2 homolog NDK-1 is required for full activation of Ras signaling in *C. elegans*. *Development*. 2013;140(16):3486-3495. doi:10.1242/dev.094011

14. Wang Y, Wang S, Nie X, et al. Molecular and structural basis of nucleoside diphosphate kinase–mediated regulation of spore and sclerotia development in the fungus *Aspergillus flavus*. *J Biol Chem*. 2019;294(33):12415-12431. doi:10.1074/jbc.RA119.007505

15. Muñoz-Dorado J, Inouye S, Inouye M. Nucleoside diphosphate kinase from *Myxococcus xanthus*. II. Biochemical characterization. *Journal of Biological Chemistry*. 1990;265(5):2707-2712. doi:10.1016/S0021-9258(19)39859-X

16. Postel EH, Berberich SJ, Rooney JW, Kaetzel DM. Human NM23/Nucleoside Diphosphate Kinase Regulates Gene Expression through DNA Binding to Nuclease-Hypersensitive Transcriptional Elements. *Journal of Bioenergetics and Biomembranes*. 2000;32(3):277–284. doi:10.1023/A:1005541114029. PMID: 11768311

17. Levit MN, Abramczyk BM, Stock JB, Postel EH. Interactions between *Escherichia coli* nucleoside-diphosphate kinase and DNA. *J Biol Chem*. 2002;277(7):5163-5167. doi:10.1074/jbc.M111170200

18. Kumar P, Verma A, Saini AK, et al. Nucleoside diphosphate kinase from *Mycobacterium tuberculosis* cleaves single strand DNA within the human c-myc promoter in an enzyme-catalyzed reaction. *Nucleic Acids Res*. 2005;33(8):2707-2714. doi:10.1093/nar/gki568

19. Coutinho-Silva R, Ojcius DM. Role of extracellular nucleotides in the immune response against intracellular bacteria and protozoan parasites. *Microbes Infect*. 2012;14(14):1271-1277. doi:10.1016/j.micinf.2012.05.009

20. Kolli BK, Kostal J, Zaborina O, Chakrabarty AM, Chang KP. *Leishmania*-released nucleoside diphosphate kinase prevents ATP-mediated cytolysis of macrophages. *Molecular and Biochemical Parasitology*. 2008;158(2):163-175. doi:10.1016/j.molbiopara.2007.12.010

21. Yilmaz Ö, Yao L, Maeda K, et al. ATP scavenging by the intracellular pathogen *Porphyromonas gingivalis* inhibits P2X7-mediated host-cell apoptosis. *Cellular Microbiology*. 2008;10(4):863-875. doi:10.1111/j.1462-5822.2007.01089.x

22. Ardissone S, Scherler A, Pillonel T, Martin V, Kebbi-Beghdadi C, Greub G. Transcriptional Landscape of *Waddlia chondrophila* Aberrant Bodies Induced by Iron Starvation. *Microorganisms*. 2020;8(12):1848. doi:10.3390/microorganisms8121848

23. Arumugam M, Ajitkumar P. Histidine 117 in the His-Gly-Ser-Asp motif is Required for the Biochemical Activities of Nucleoside Diphosphate Kinase of *Mycobacterium smegmatis*. *Open Biochem J*. 2012;6:71-77. doi:10.2174/1874091X01206010071

24. Singh S, Yadav PK, Singh AK. In-silico structural characterization and phylogenetic analysis of Nucleoside diphosphate kinase: A novel antiapoptotic protein of *Porphyromonas gingivalis*. *Journal of Cellular Biochemistry*. 2023;124(4):545-556. doi:10.1002/jcb.30389

25. Janin J, Dumas C, Moréra S, et al. Three-Dimensional Structure of Nucleoside Diphosphate Kinase. *J Bioenerg Biomembr*. 2000;32(3):215-225. doi:10.1023/A:1005528811303

26. Kamath S, Chen ML, Chakrabarty AM. Secretion of Nucleoside Diphosphate Kinase by Mucoid *Pseudomonas aeruginosa* 8821: Involvement of a Carboxy-Terminal Motif in Secretion. *J Bacteriol*. 2000;182(13):3826-3831.

27. Neeld D, Jin Y, Bichsel C, et al. *Pseudomonas aeruginosa* injects NDK into host cells through a type III secretion system. *Microbiology (Reading)*. 2014;160(Pt 7):1417-1426. doi:10.1099/mic.0.078139-0

28. Atanasova K, Lee J, Roberts J, Lee K, Ojcius DM, Yilmaz Ö. Nucleoside-Diphosphate-Kinase of *P. gingivalis* is Secreted from Epithelial Cells in the Absence of a Leader Sequence Through a Pannexin-1 Interactome. *Scientific Reports*. 2016;6(1). doi:10.1038/srep37643

29. Kebbi-Beghdadi C, Pilloux L, Martin V, Greub G. Eukaryotic Cell Permeabilisation to Identify New Putative Chlamydial Type III Secretion System Effectors Secreted within Host Cell Cytoplasm. *Microorganisms*. 2020;8(3):361. doi:10.3390/microorganisms8030361

30. Ouellette SP, Blay EA, Hatch ND, Fisher-Marvin LA. CRISPR Interference to Inducibly Repress Gene Expression in *Chlamydia trachomatis*. *Infect Immun*. 89(7):e00108-21. doi:10.1128/IAI.00108-21

31. Yahr TL, Wolfgang MC. Transcriptional regulation of the *Pseudomonas aeruginosa* type III secretion system. *Molecular Microbiology*. 2006;62(3):631-640. doi:10.1111/j.1365-2958.2006.05412.x

32. Valenti D, Barile M, Quagliariello E, Passarella S. Inhibition of nucleoside diphosphate kinase in rat liver mitochondria by added 3′-azido-3′-deoxythymidine. *FEBS Letters*. 1999;444(2-3):291-295. doi:10.1016/S0014-5793(99)00071-X

33. Schaertl S, Konrad M, Geeves MA. Substrate Specificity of Human Nucleoside-diphosphate Kinase Revealed by Transient Kinetic Analysis. *Journal of Biological Chemistry*. 1998;273(10):5662-5669. doi:10.1074/jbc.273.10.5662

34. Gallois-Montbrun S, Schneider B, Chen Y, et al. Improving Nucleoside Diphosphate Kinase for Antiviral Nucleotide Analogs Activation. *Journal of Biological Chemistry*. 2002;277(42):39953-39959. doi:10.1074/jbc.M206360200

35. Xu Y, Sellam O, Moréra S, et al. X-ray analysis of azido-thymidine diphosphate binding to nucleoside diphosphate kinase. *Proceedings of the National Academy of Sciences*. 1997;94(14):7162-7165. doi:10.1073/pnas.94.14.7162

36. Wambaugh MA, Shakya VPS, Lewis AJ, Mulvey MA, Brown JCS. High-throughput identification and rational design of synergistic small-molecule pairs for combating and bypassing antibiotic resistance. *PLOS Biology*. 2017;15(6):e2001644. doi:10.1371/journal.pbio.2001644

37. Furman PA, Barry DW. Spectrum of antiviral activity and mechanism of action of zidovudine. An overview. *Am J Med*. 1988;85(2A):176-181.

38. Adams NE, Thiaville JJ, Proestos J, et al. Promiscuous and Adaptable Enzymes Fill "Holes" in the Tetrahydrofolate Pathway in Chlamydia Species. *mBio*. 2014;5(4):e01378-14. doi:10.1128/mBio.01378-14

39. Dille S, Kleinschnitz EM, Kontchou CW, Nölke T, Häcker G. In contrast to *Chlamydia trachomatis*, *Waddlia chondrophila* grows in human cells without inhibiting apoptosis, fragmenting the Golgi apparatus, or diverting post-Golgi sphingomyelin transport. *Infect Immun*. 2015;83(8):3268-3280. doi:10.1128/IAI.00322-15

40. Croxatto A, Greub G. Early intracellular trafficking of *Waddlia chondrophila* in human macrophages. *Microbiology (Reading)*. 2010;156(Pt 2):340-355. doi:10.1099/mic.0.034546-0

41. Pillonel T, Tagini F, Bertelli C, Greub G. ChlamDB: a comparative genomics database of the phylum Chlamydiae and other members of the Planctomycetes-Verrucomicrobiae-Chlamydiae superphylum. *Nucleic Acids Research*. 2020;48(D1):D526-D534. doi:10.1093/nar/gkz924

42. Kelley LA, Mezulis S, Yates CM, Wass MN, Sternberg MJE. The Phyre2 web portal for protein modeling, prediction and analysis. *Nat Protoc*. 2015;10(6):845-858. doi:10.1038/nprot.2015.053

43. Mueller KE, Wolf K, Fields KA. *Chlamydia trachomatis* transformation and allelic exchange mutagenesis. *Curr Protoc Microbiol*. 2017;45:11A.3.1-11A.3.15. doi:10.1002/cpmc.31

FIGURES

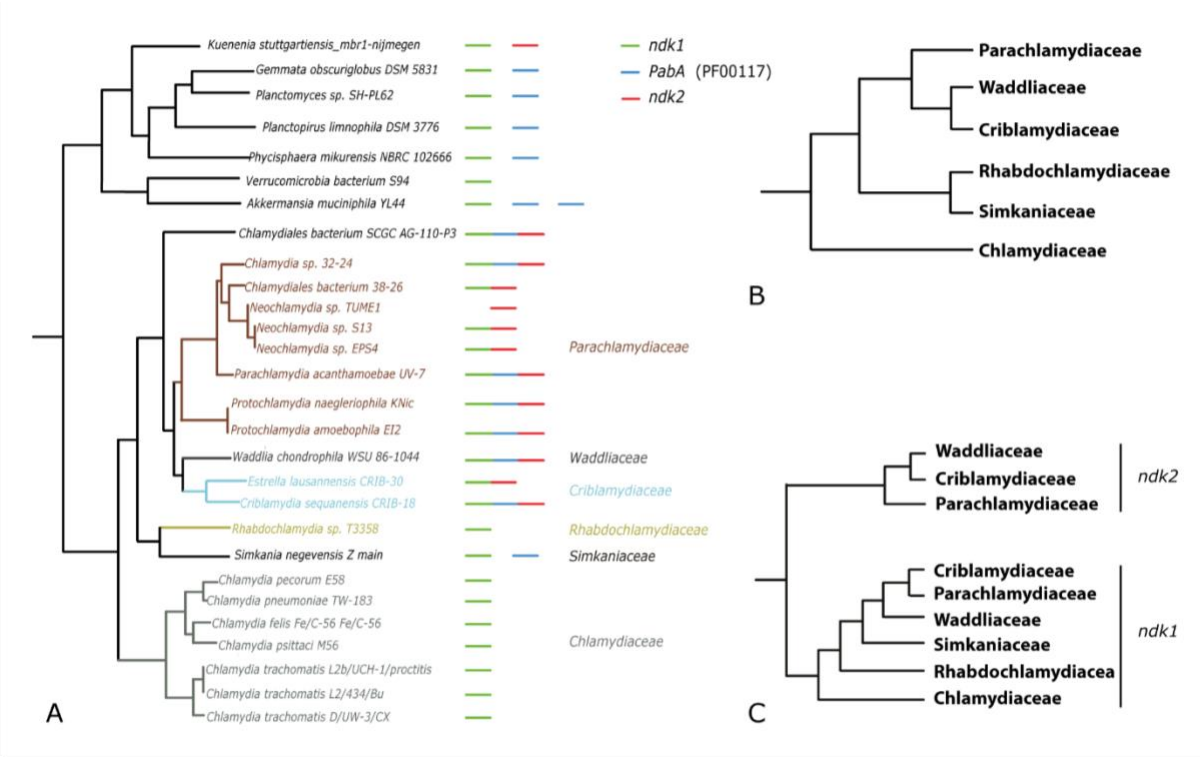

Figure1: Phylogeny of *Chlamydiota* phylum and the *ndk* gene operon evolution. (A) Species phylogeny based on 32 single-copy orthologous genes. (B) Simplified representation of the species phylogeny highlighting major clades. (C) Phylogeny based on the *ndk* gene, showing its evolutionary relationship among *Chlamydial* species.

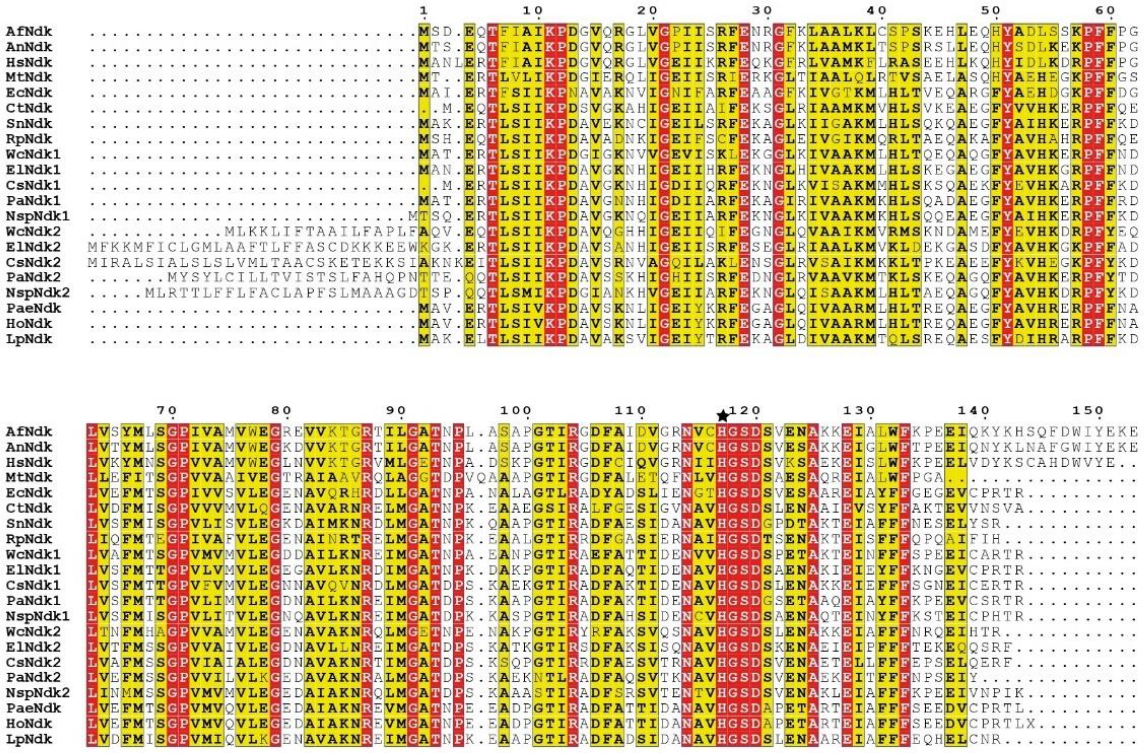

A

	WcNdk1	WcNdk2	CtNdk	EcNdk	MtNdk
WcNdk2	54%				
CtNdk	66%	59%			
EcNdk	67%	49%	63%		
MtNdk	57%	48%	54%	56%	
HsNdk	53 %	44 %	51%	52%	52%

B

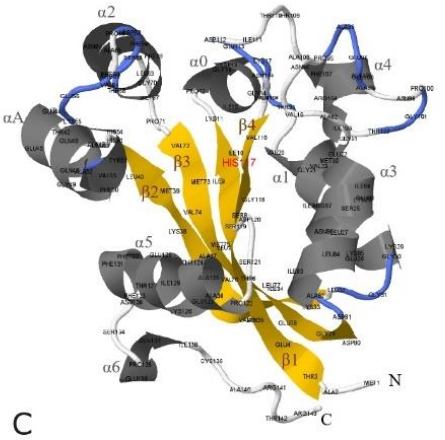

C

Figure 2: Ndk sequence and structure conservation. (A) Multiple sequence alignment of Ndk proteins across eukaryotes and prokaryotes. Conserved residues are highlighted in red with the highly conserved H residue, essential for catalytic activity, marked with an asterisk. Af: *Aspergillus flavus*, An: *A. niger*, Hs: *Homo sapiens*, Mt: *Mycobacterium tuberculosis*, Ec: *Escherichia coli,* Ct: *C. trachomatis*, Sn: *Simkania negevensis*, Rp: *Rhabdochlamydia porcellionis,* Wc: *W. chondrophila*, El: *Estrella lausannensis,* Cs: *Criblamydia sequanensis,* Pa: *Parachlamydia acanthamoebae,* Nsp: *Neochlamydia sp.*, Pae: *Pseudomonas aeruginosa*, Ho: *Halofilum ochraceum*, Lp: *Legionella pneumophila* (B) Amino acid sequence similarity matrix comparing Ndk proteins from *W. chondrophila* (WcNdk1 and WcNdk2), *Chlamydia trachomatis* (CtNdk), *Escherichia coli* (EcNdk), *Mycobacterium tuberculosis* (MtNdk), and human Ndk (HsNdk). (C) Predicted 3D structure of WcNdk1, illustrating its conserved α/β fold characteristic of the Ndk family. 3D structure reconstructed using Phyre2 and visualized using Jmol v.16.2.15. The H177, highlighted in red, is a critical histidine residue and positioned within the active site.

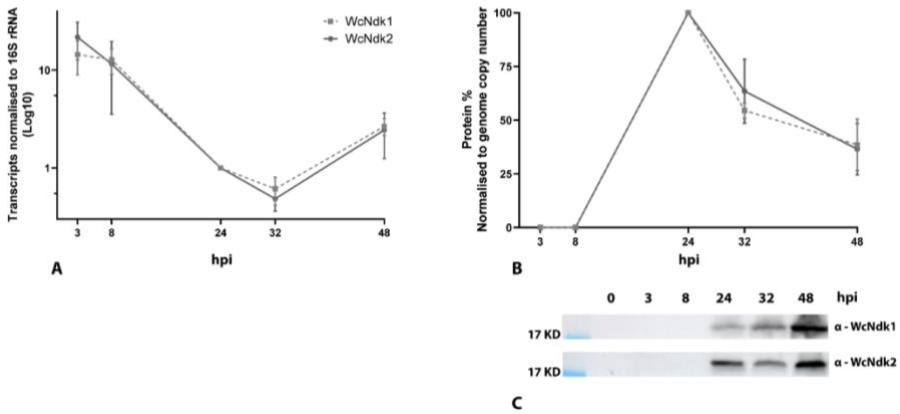

Figure 3: Temporal expression analysis of *ndk* paralogs in *W. chondrophila* during infection. (A) Quantitative RT-PCR analysis of *ndk1* and *ndk2* transcript levels at different hours post-infection (hpi), normalized to 16S rRNA. Transcript abundance is expressed relative to the 24 hpi time point, which was set as the reference (1.0). (B) Relative protein levels of WcNdk1 and WcNdk2 quantified by Western blot, normalized to bacterial genome copy number. Protein expression is shown relative to 24 hpi, set as 100%. (C) Representative Western blot images showing WcNdk1 and WcNdk2 expression across the infection time course. Data are shown as mean ± SD of 3 independent experiments.

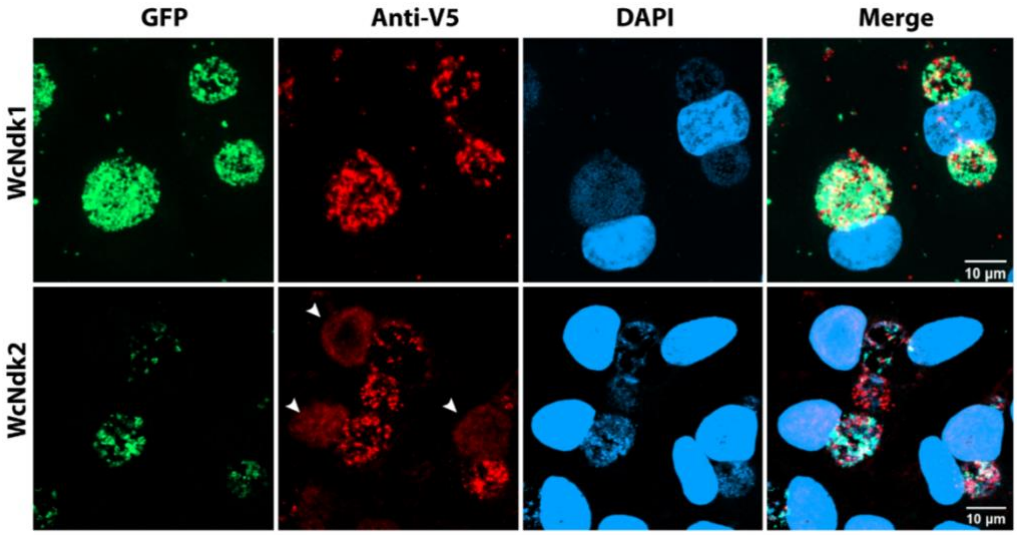

Figure 4: Subcellular localization of WcNdk1 and WcNdk2 overexpressed in *C. trachomatis*. *C. trachomatis* was transformed with plasmids expressing either WcNdk1 or WcNdk2 tagged with a V5 epitope. Infected McCoy cells were fixed at 24 hpi. GFP (green) indicates transformed *C. trachomatis*, anti-V5 (red) detects WcNdk proteins, and DAPI (blue) stains host cell nuclei and bacterial DNA. White arrows point to V5 signal within host nuclei.

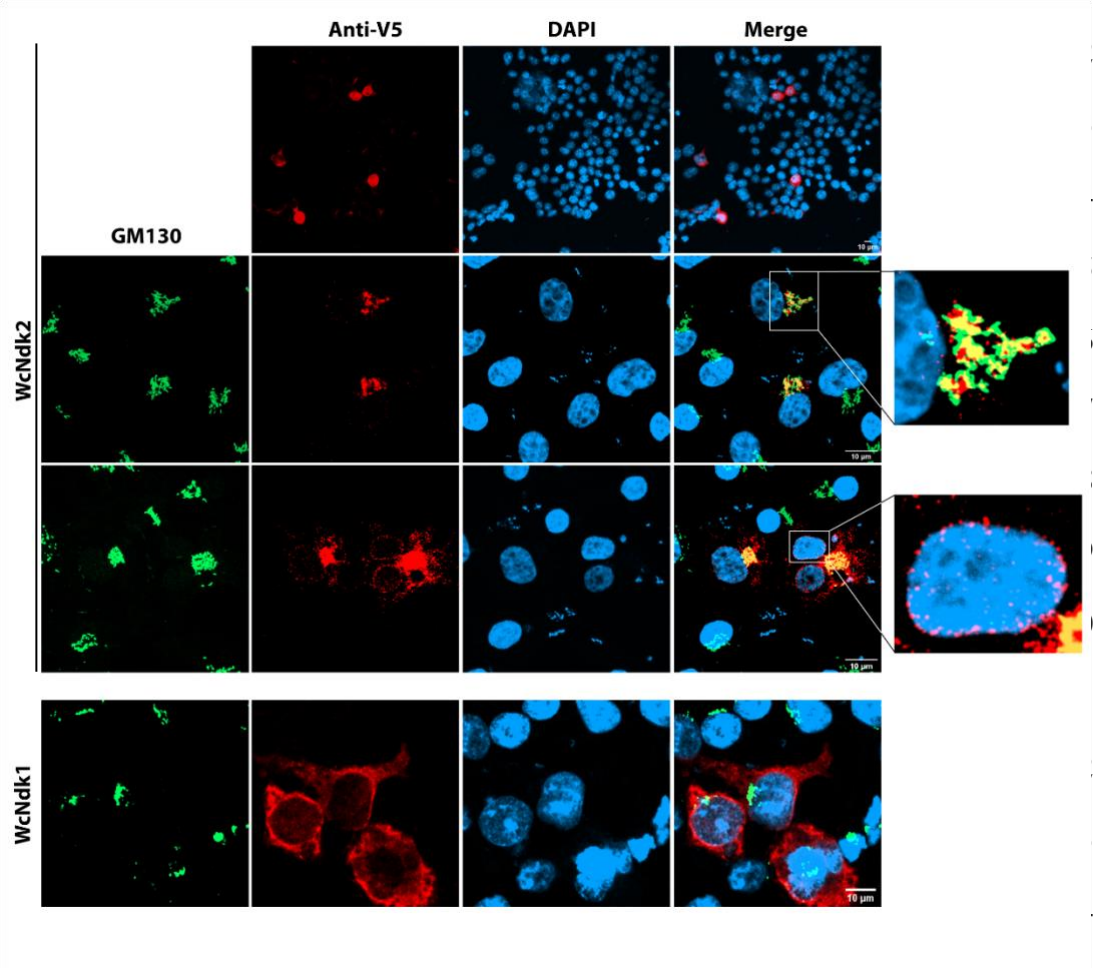

Figure 5: Subcellular distribution of WcNdk1 and WcNdk2 in HEK293T. HEK293T cells were transiently transfected with C-terminal V5-tagged WcNdk1 and WcNdk2 and stained with the Golgi marker GM130 (green), anti-V5 antibody (red), and DNA (DAPI, blue). High-magnification insets highlight the co-localization of WcNdk2 (red) with the Golgi (green) or the perinuclear region.

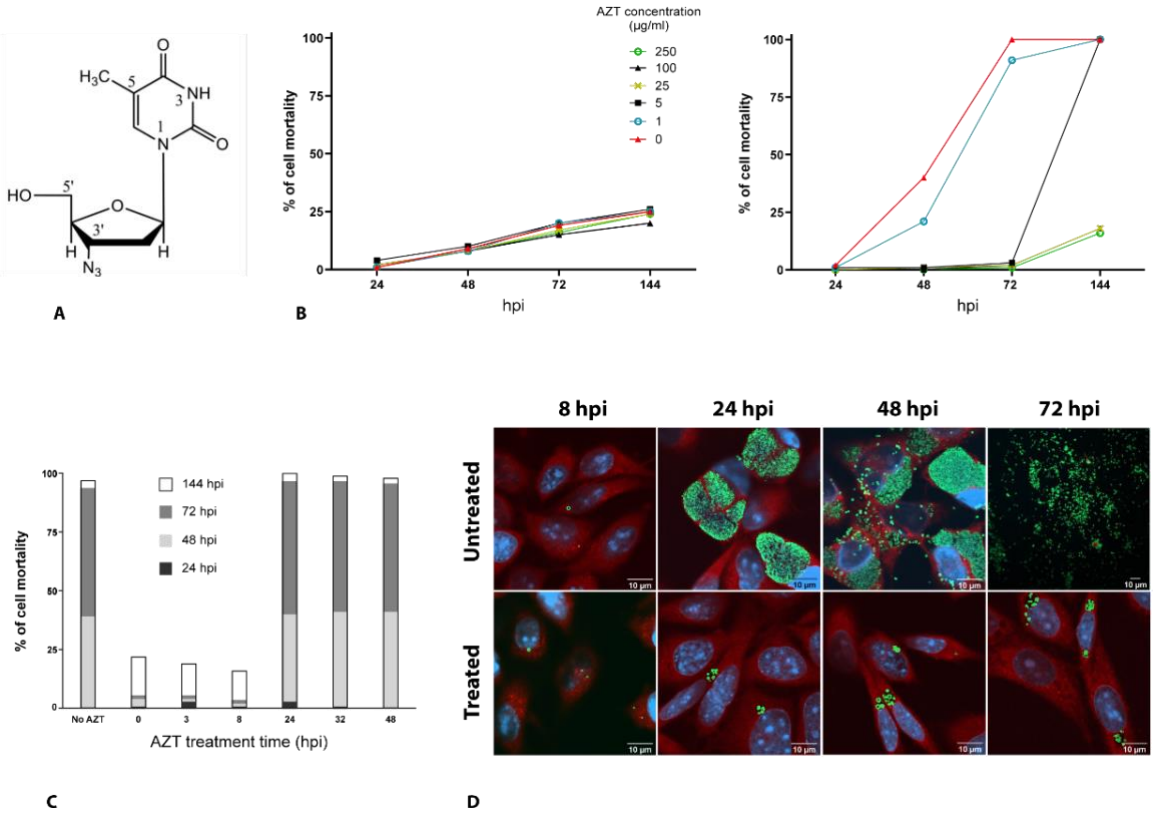

Figure 6: AZT inhibits *W. chondrophila* growth in infected host cells. (A) Chemical structure of azidothymidine (AZT). (B) AZT treatment of uninfected host cells, serving as a negative control (left panel) and treatment of infected host cells at concentrations ≥25 µg/mL (right panel). (C) Effect of AZT addition on *W. chondrophila*-infected cultures at various time points after infection. (D) Confocal microscopy of *W. chondrophila*-infected cells treated or not treated with AZT. In untreated conditions, *W. chondrophila* formed typical intracellular inclusions, whereas AZT treatment resulted in enlarged, aberrant structures. Bacteria are labeled using anti-*W. chondrophila* antibody (green); host cell nuclei are stained with DAPI (blue); and the host structures are marked with Concanavalin A (red).

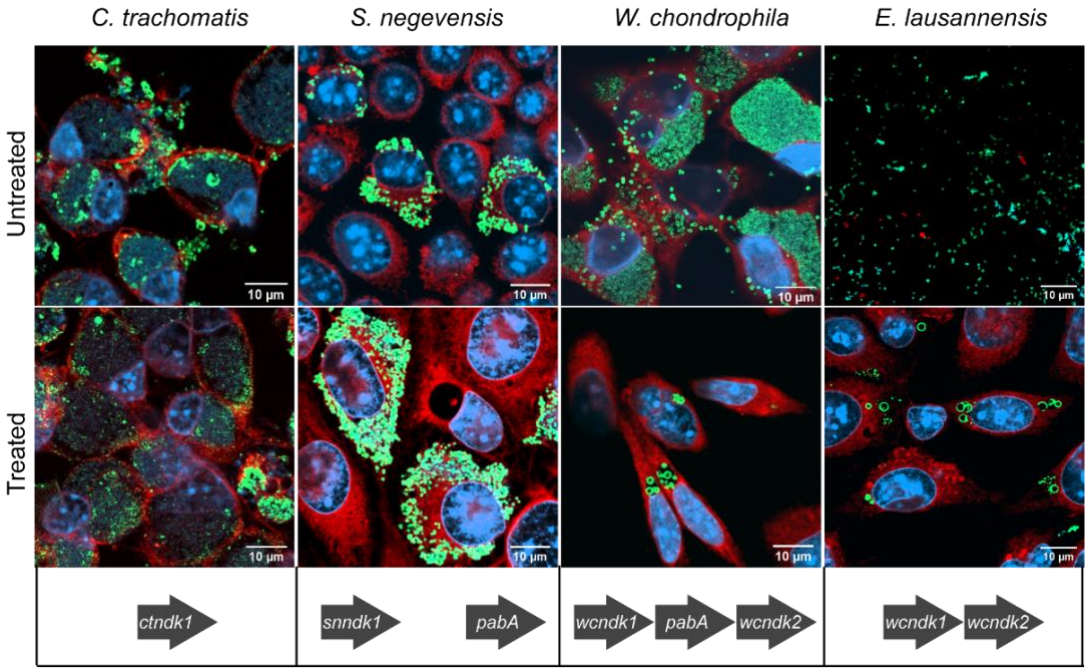

Figure 7: AZT sensitivity is restricted to *Chlamydiota* species encoding *ndk2*. Representative confocal micrographs of McCoy cells infected with *C. trachomatis*, *S. negevensis*, *W. chondrophila* or *E. lausannensis*, treated or not treated with 25 µg/ml AZT. The infected cells were fixed and stained 48 hpi. The lower panel shows the *ndk* operon arrangement: *C. trachomatis* and *S. negevensis*, each carry a single *ndk* gene. *S. negevensis* retains *pabA* elsewhere in the genome. *W. chondrophila* carries the two *wcndk* genes with a *pabA* in the middle. *E. lausannensis* encodes a two-gene *elndk1–elndk2* operon but lacks *pabA*. Bacteria are stained with species-specific antibodies. Host cytoplasm is labeled with Concanavalin A (red), and nuclei are stained with DAPI (blue). *ctndk*: *C. trachomatis ndk1*, *snndk1*: *S. negevensis ndk1*, *elndk1*: *E. lausannensis ndk1*, *elndk2*: *E. lausannensis ndk2.*

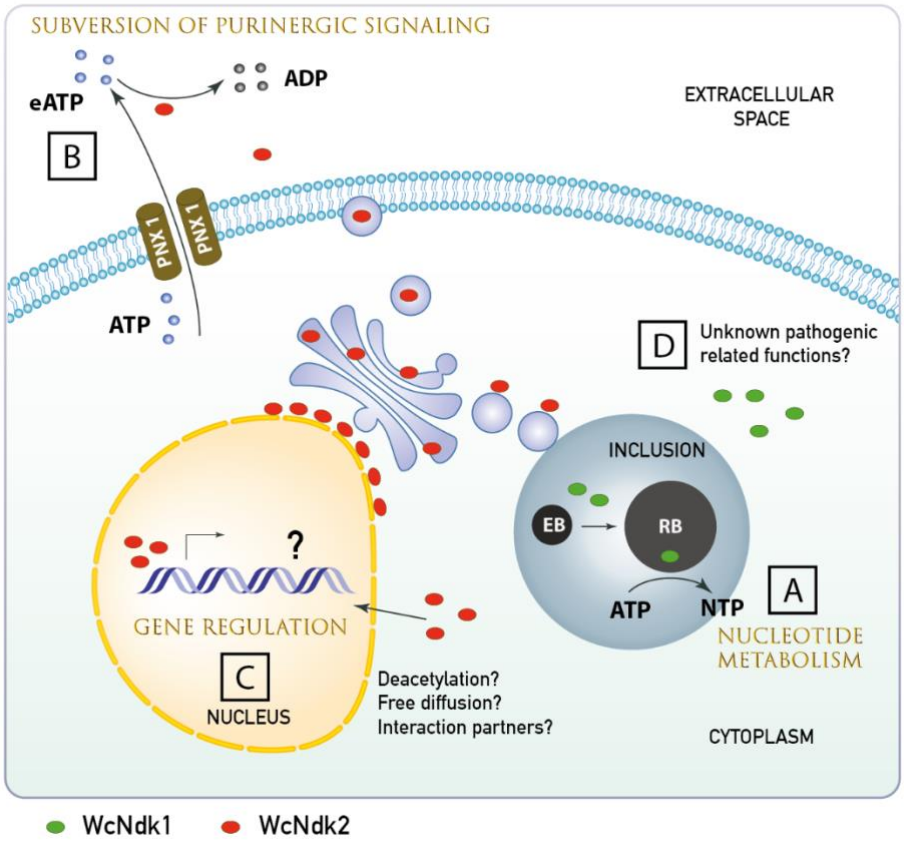

Figure 8: Proposed model for the functions of WcNdk1 and WcNdk2 in *W. chondrophila.* This schematic illustrates the distinct subcellular localizations and putative roles of WcNdk1 (green) and WcNdk2 (red), during infection of a host cell. A: WcNdk1 is predominantly retained within the bacterial inclusion, where it sustains basic nucleotide metabolism and "housekeeping" functions. B: A fraction of WcNdk1 is secreted across the inclusion membrane into the host cytosol, however, the specific functions of cytosolic WcNdk1 remain undefined. C: WcNdk2 is observed accumulating within the host nucleus. Its import into the nucleus could occur via one or more of the following mechanisms: a deacetylation event allowing passive nuclear import; free diffusion through nuclear pores owing to its small molecular size; or interaction with host proteins that escort WcNdk2 into the nucleus. Inside host nucleus, WcNdk2 could bind directly to DNA leading to up- or downregulation of host genes involved in immunity or apoptosis. The precise gene targets remain unknown. D: WcNdk2 traffics through Golgi/ER-derived vesicles and perinuclear region. This localization may be related to the packaging of WcNdk2 into vesicles destined for secretion to subvert host purinergic signaling through hydrolysis of eATP into ADP. E: The association of WcNdk2 with the Golgi apparatus may imply an involvement in vesicle trafficking and acquisition of host-derived metabolites necessary for expansion of the inclusion and bacterial survival. Illustration generated using Adobe Illustrator 2024 (Adobe Inc., USA).